

Glass Transition Temperature of Glucose, Sucrose, and Trehalose: An Experimental and in Silico Study

Alexandra Simperler,[†] Andreas Kornherr,^{*,‡} Reenu Chopra,[†] P. Arnaud Bonnet,[†]
William Jones,^{*,†} W. D. Samuel Motherwell,[§] and Gerhard Zifferer[‡]

The Pfizer Institute for Pharmaceutical Materials Science, Department of Chemistry, University of Cambridge, Lensfield Road, Cambridge CB2 1EW, United Kingdom, Institute of Physical Chemistry, University of Vienna, Währinger Strasse 42, A-1090 Wien, Austria, and The Pfizer Institute for Pharmaceutical Materials Science, Cambridge Crystallographic Database Centre, 12 Union Road, Cambridge CB2 1EZ, United Kingdom

Received: May 22, 2006; In Final Form: July 13, 2006

Isothermal–isobaric molecular dynamics simulations are used to calculate the specific volume of models of different amorphous carbohydrates (glucose, sucrose, and trehalose) as a function of temperature. Plots of specific volume vs temperature exhibit a characteristic change in slope when the amorphous systems change from the glassy to the rubbery state. The intersection of the regression lines of data below (glassy state) and above (rubbery state) the change in slope provides the glass transition temperature (T_g). These predicted glass transition temperatures are compared to experimental T_g values as obtained from differential scanning calorimetry measurements. As expected, the predicted values are systematically higher than the experimental ones (about 12–34 K) as the cooling rates of the modeling methods are about a factor of 10^{12} faster. Nevertheless, the calculated trend of T_g values agrees exactly with the experimental trend: $T_g^{\text{glucose}} < T_g^{\text{sucrose}} < T_g^{\text{trehalose}}$. Furthermore, the relative differences between the glass transition temperatures were also computed precisely, implying that atomistic molecular dynamics simulations can reproduce trends of T_g values in amorphous carbohydrates with high quality.

1. Introduction

The amorphous state is omnipresent within the pharmaceutical and food industries^{1–3} as a great amount of organic compounds, such as proteins and peptides, do not easily crystallize. The amorphous state of an inactive compound (excipient) may even be deliberately produced by standard processes³ to effectively encapsulate, stabilize, and release labile pharmaceutically active materials. For example, carbohydrates find use as excipients⁴ due to their advantageous properties which include being good glass-formers and having high glass transition temperatures (T_g). The disaccharides sucrose and trehalose are often used in stabilizing membranes and proteins,^{4,5} either in their pure form or as part of an excipient mixture. Trehalose is widely used because of its relatively high T_g and low tendency to crystallize.^{4–6}

The glass transition temperatures are related to the physical stability of an amorphous formulation;⁴ below the T_g , pharmaceutically active materials should be stable due to high viscosity. The structural relaxation time of a system slows dramatically at the T_g , and thus, the molecular mobility becomes extremely reduced. Different factors such as added buffers, salts, and moisture can depress the glass transition temperatures. Thus, it is very important to use excipients that have a high T_g to compensate for these possible factors. The pharmaceutical industry, therefore, makes great efforts to design elaborate excipient mixtures to optimize encapsulation, storage, and release of a drug.

Computational methods can be used to assist in tailoring new excipient mixtures. Models of excipient mixtures can be built in silico, and the quality of physical stabilization can be estimated by calculating the T_g with respect to the ratio of components. Other important challenges for modelers are the influence of water (i.e., from humidity) on the stability of excipients and the interactions between pharmaceutically active compounds and excipients. Before attempting to use modeling directly on complex models, the T_g values of the three well-known glass-forming carbohydrates glucose, sucrose, and trehalose (Figure 1) have been calculated and compared to experimental data obtained from differential scanning calorimetry (DSC) measurements. Sucrose and trehalose have been selected because, as mentioned above, they are used in the pharmaceutical industry as excipients. Despite less importance as an excipient, the simple monosaccharide glucose has been chosen as a further less complex testing case.

The accuracy of an in silico method can only be established when experimental values are available to be compared to calculated values, and only then can a method be used with confidence in predicting values. The chosen in silico method for calculating glass transition temperatures is to simulate the cooling of an amorphous solid by performing isothermal–isobaric molecular dynamics at set temperatures.

The thermal expansivity of an amorphous system is expected to decrease at its T_g when it passes from a rubbery to a glassy state. Thus, a plot of the specific volume (v_{spec}) vs temperature for an amorphous system will be expected to show a change in slope at the glass transition. The T_g can thus be identified as the point of intersection between the high- and low-temperature branches in this plot. Often in modeling, this method is used to determine the T_g of polymers^{7–11} and carbohy-

* To whom correspondence should be addressed. (A.K.) E-mail: andreas.kornherr@univie.ac.at. Phone: +43 (0) 1-4277-52434. (W.J.) E-mail: wj10@cam.ac.uk. Phone: +44 (0) 1223-336468.

[†] University of Cambridge.

[‡] University of Vienna.

[§] Cambridge Crystallographic Database Centre.

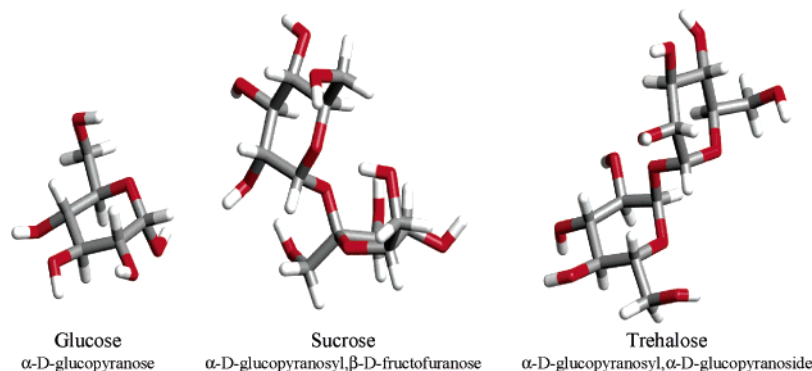


Figure 1. Models of glucose, sucrose, and trehalose.

drates,^{12–20} and there is also experimental evidence^{21,22} confirming that the specific volume indeed shows a change in slope at its T_g . Thus, we follow the so-called free volume theory.^{23,24} However, it should be acknowledged that at this time it is not absolutely clear whether the (free) volume and the density or the temperature^{25,26} are the main controlling parameters determining the dramatic slowing of the structural relaxation times at the T_g .²⁷

Using molecular dynamics (MD) is likely to give an overestimate of the T_g values.²⁸ The measurement of a T_g is highly dependent on the cooling rate,²⁹ which is in the range of minutes in an experiment such as DSC. In contrast, the cooling rate in an MD study is in the nanosecond range. Thus, the calculated T_g values cannot be expected to be quantitatively similar to the T_g values obtained from DSC measurements. However, we will show that the calculated T_g values are in the same order as the experimental values: $T_g^{\text{glucose}} < T_g^{\text{sucrose}} < T_g^{\text{trehalose}}$. Furthermore, the incremental changes of the modeled set of T_g values are comparable to the experimental one.

2. Methods

2.1. Experimental Methods. The three carbohydrates were commercially obtained as crystalline powders: α -D-glucose from Arcos Organics ($\geq 99\%$ purity), sucrose from Aldrich ($\geq 98\%$ purity), and α,α -D-(+)-trehalose dihydrate from Fluka ($\geq 99.0\%$ purity). The glassy state of glucose was obtained experimentally via quench-cooling. The sample was equilibrated at 303 K for 1 min and then cooled to 243 K at a rate of 10 K/min. Subsequently, the sample was melted by raising the temperature to 436 K and quench-cooled again to 243 K. To obtain amorphous sucrose and trehalose samples, freeze-drying was performed using a VirTis AdvAntage benchtop freeze-dryer. The freeze-dried sugar samples (5–10 mg) were placed in DSC pans and were sealed inside a glovebox, which was kept at a relative humidity below 0.5% using regenerated molecular sieves.

For all DSC measurements, a Mettler Toledo STAR DSC822^e differential scanning calorimeter was used with nitrogen purge at 50 cm³/min. An indium calibration was used ($T_m = 429.60 \pm 0.3$ K, heat of fusion 28.45 ± 0.6 J/g), and the samples (ca. 2–10 mg) were analyzed in crimped aluminum pans (40 and 100 μ L).

From the heat cycles, a T_g (referred to as T_g^{mid}) for each of the three carbohydrates was obtained as the midpoint²⁹ of an endothermic transition. A second T_g (referred to as T_g^{cool}) was obtained by integrating the experimental cooling curves. The resulting plot shows a change of slope, and the intersection of the regression lines of data above and below the change in slope results in the glass transition temperature T_g^{cool} .

2.2. Theoretical Methods. The molecular structures of glucose, sucrose, and trehalose were extracted from the Cambridge Structural Database (CSD).^{30,31} We considered no specific conformers of the molecules, and all structures were kept fully flexible during the whole MD process. Subsequently, the amorphous model systems of the carbohydrates were built with the Amorphous Cell tool as implemented in the Materials Studio 3.0 simulation package from Accelrys.³² A total of 144 molecules of glucose and 72 molecules of the disaccharide sucrose or trehalose were used to build cubic amorphous cells with dimensions close to $3.0 \times 3.0 \times 3.0$ nm. In total, three models were built for each of the saccharides, and thus, three independent data sets were available for the determination of a glass transition temperature.

These periodic cells were relaxed for 2 ns under isobaric–isothermal conditions (NPT ensemble) at a temperature of about 100 K above the experimental T_g values (i.e., 420, 430, and 470 K for glucose, sucrose, and trehalose, respectively). The final configurations of these MD runs were used as starting structures for a cooling cycle where the temperature was decreased in 10 K steps until a temperature about 100 K below the experimental T_g value was reached (i.e., 220, 230, and 270 K for glucose, sucrose, and trehalose). At each temperature, an NPT MD run was carried out for 200 ps, where 150 ps allows for equilibration at the particular temperature and the last 50 ps is used for data sampling. The final configuration of each individual 200 ps run served as the starting structure for the subsequent one. For the last 50 ps, at every picosecond the specific density (ρ_{spec}) was sampled, and the average value (over these 50 data points) was taken as the result. Plots of ρ_{spec} vs simulation time (t) (Figure 2) for each of the saccharides (for three different temperatures) show that all ρ_{spec} values are well equilibrated within the chosen simulation period of 200 ps. v_{spec} can subsequently be calculated via $1/\rho_{\text{spec}}$, and these specific volumes were plotted vs temperature.

In the case of glucose, heating cycles were also performed; the final configurations of the three cooling cycles (i.e., the configurations at 220 K) were relaxed for 2 ns under isobaric–isothermal conditions. The three resulting relaxed configurations were entered into the heating cycles. For the relaxation process as well as for the subsequent cooling and heating cycles, MD simulations were performed with DISCOVER³² using the COMPASS^{33–36} force field. The Anderson thermostat and barostat³⁷ were employed with a time step of 1 fs. Since the internal pressure of a solid or liquid compound exceeds the external pressure by 3–4 orders of magnitude, the external pressure can be set to zero for convenience (preliminary calculations showed that accounting for the external pressure of 10^5 Pa the specific volume is only changed by less than

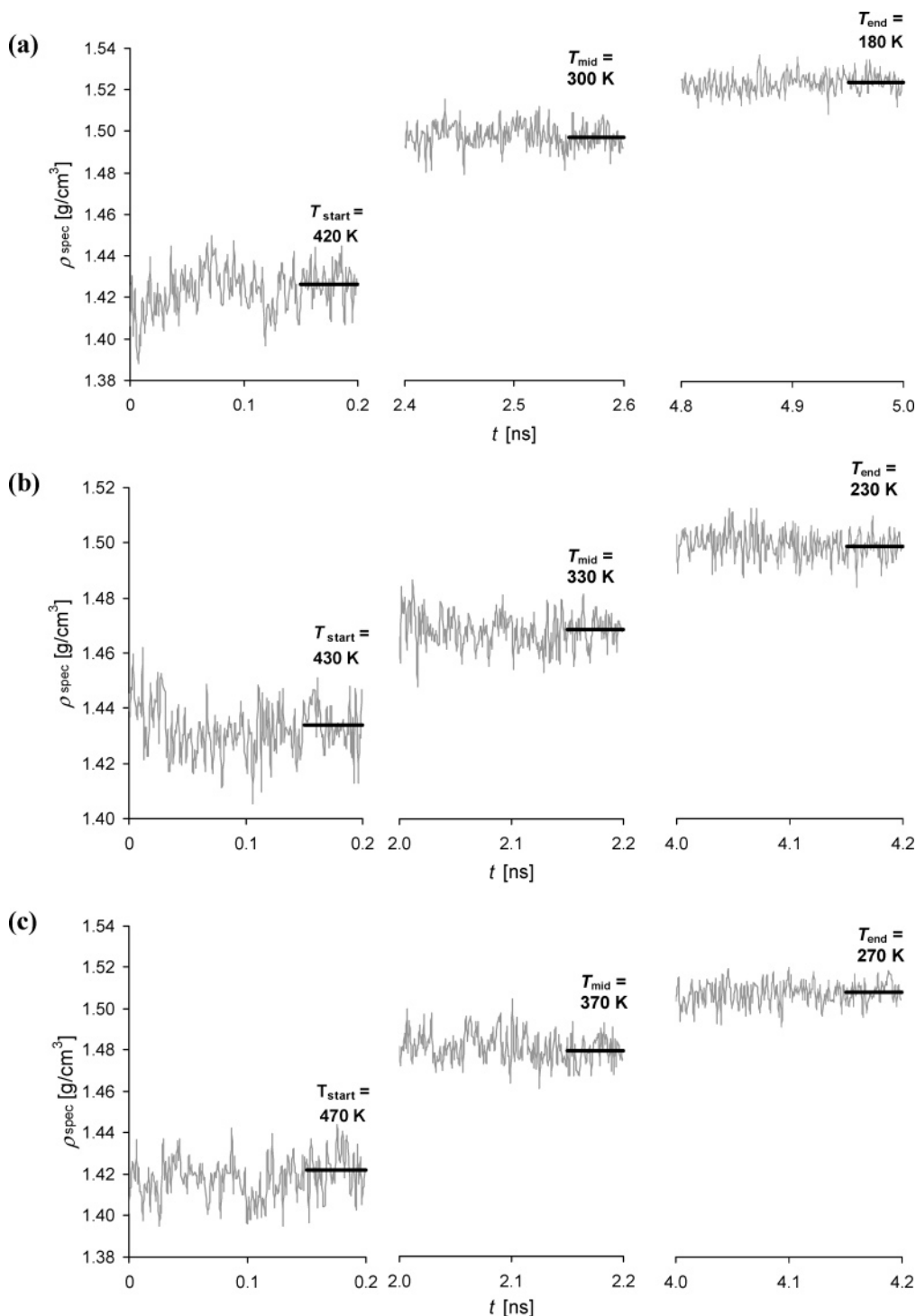


Figure 2. ρ_{spec} vs t for (a) glucose, (b) sucrose, and (c) trehalose for three different temperatures: start temperature (T_{start}), midpoint temperature (T_{mid} ; near T_g), and end temperature (T_{end}). The average ρ_{spec} values over the last 50 ps (visualized by bold lines) are given within the figure.

0.2%—which is by far smaller than normal fluctuations of this key property). The cutoffs (with a cutoff radius of 1.25 nm) for the computation of energies and forces for the electrostatic as well as van der Waals interactions (employing a Lennard-Jones 9–6 function) were charge group based to avoid erroneous monopole–monopole terms. The calculation for glucose was also done once using the Ewald summation to check the applicability of the chosen cutoff radius; the discrepancies with respect to the calculated specific volumes were less than 1%, but the charged group based summation enhanced the computing speed by a factor of approximately 15.

3. Results

3.1. Isobaric–Isothermal Molecular Dynamic Simulations.

We consider the procedure of obtaining T_g with isobaric–isothermal MD calculations in more detail using the example of glucose (Figure 3). v_{spec} of all three amorphous models (referred to as models A, B, and C, open symbols) is plotted vs temperature in the upper plot (Figure 3). If these data points were connected, a curve with a shallow flexion would be obtained. As mentioned above, this is due to the different linear relationships between v_{spec} and temperature at temperatures below and above the glass transition temperature. Above the

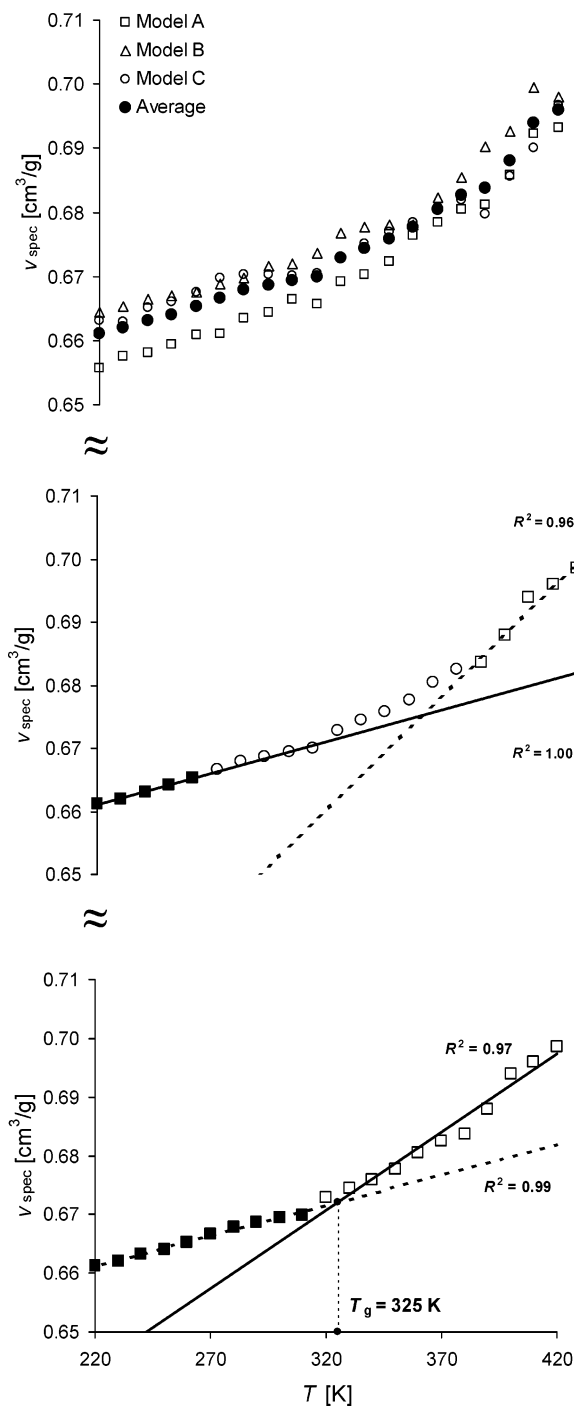


Figure 3. Calculated v_{spec} vs T plots of glucose. Upper plot: v_{spec} data of three independent models of amorphous glucose (open symbols) along with average v_{spec} data (closed symbols). Middle plot: fit of two linear regression lines through the first five v_{spec} data points of the glassy branch (■) and the last five points of the rubbery branch (□). Nonallocated points are indicated with ○. Lower plot: fit of two linear regression lines through the v_{spec} data points of the glassy branch (solid line) and the data points of the rubbery branch (dashed line). T_g is indicated at their intersection. R^2 of the linear regressions in this and the following figures is directly given in the plots.

glass transition in the rubbery phase the specific volume will increase more rapidly with increasing temperature than in the glassy phase, and this phenomenon of a change in the slope will be used for determining T_g . The upper plot in Figure 3 also shows that in the glassy phase fluctuations are less pronounced than at higher temperatures (i.e., in the rubbery phase), where the data points are more scattered. This is

probably caused by the higher kinetic energy associated with higher temperature. A sharp improvement, however, could be reached by taking the average over the three data sets (closed symbols, Figure 3, upper plot), where the data points especially at higher temperatures are less scattered.

Thus, the average v_{spec} vs temperature (Figure 3, middle plot) is used to determine the T_g . The difficulty now lies in separating the data points into a glassy and rubbery phase. We can confidently assume that the five data points at lowest temperature (■, Figure 3, middle plot) belong to the glassy state whereas the five high-temperature points (□, Figure 3, middle plot) belong to the rubbery state. A linear regression line through each of these two sets of five points allows a correlation coefficient (R^2) value to be calculated. The remaining points (○, Figure 3, middle plot) then have to be allocated to either the glassy or the rubbery phase. Whenever a new data point is added, the quality of its allocation is roughly checked by monitoring the changes of R^2 values of the corresponding linear regression line. When all data points are successfully separated into a glass and a rubber set, the intersection of the two resulting linear regression lines indicates the change of slope of the v_{spec} vs T plot (Figure 3, lower plot), thus yielding a T_g value of 325 K.

The same procedure has been applied to sucrose (Figure 4a) and trehalose (Figure 4b). The data of the two disaccharides are more scattered (Figure 4, upper plots) than those of glucose. However, the average over the three individual data sets results in a reasonable v_{spec} vs T plot, and the corresponding T_g value can be obtained from the intersecting linear regression lines (Figure 4, lower plots): 347 K for sucrose and 392 K for trehalose.

3.2. Comparison of Experimental and Calculated T_g Values. Commonly, experimentalists determine T_g by monitoring the heat capacity (C_p) using DSC. The heat capacity is the change of the enthalpy (H) of a system with respect to temperature:³⁸

$$C_p = \partial H(T)/\partial T \quad (1)$$

Typical heating traces from DSC runs show an endothermic peak (endothermic overshoot) due to physical aging phenomena (enthalpic relaxation) near the glass transition,^{6,29,39–41} whereas the cooling traces show a “smooth” transition. The glass transition temperature is usually characterized²⁹ as the midpoint of the endothermic transition in a heat cycle, referred to as T_g^{mid} . The T_g^{mid} values for glucose, sucrose, and trehalose are 296, 333, and 380 K, respectively.

The integral over an experimentally obtained DSC heating or cooling trace

$$\int C_p dT = H(T) + \text{constant} \quad (2)$$

can also be used to determine glass transition temperatures. The resulting H (shorthand for $H(T) + \text{constant}$) vs temperature plots are essentially curves with inflections in the glass transition region. The experimental glass transition temperature is obtained by fitting regression lines through the low and high-temperature branches of these curves, and determining their intersections. Integrals over cooling traces result in curves with a shallow inflection which graphically resemble the v_{spec} vs T plots as obtained from calculations. For this reason and since actual cooling cycles have been modeled, the experimental glass transition temperature T_g^{cool} was obtained by integrating cooling curves. Notably, integrals over heating traces have a bulge³⁸ on top of this shallow inflection due to the endothermic

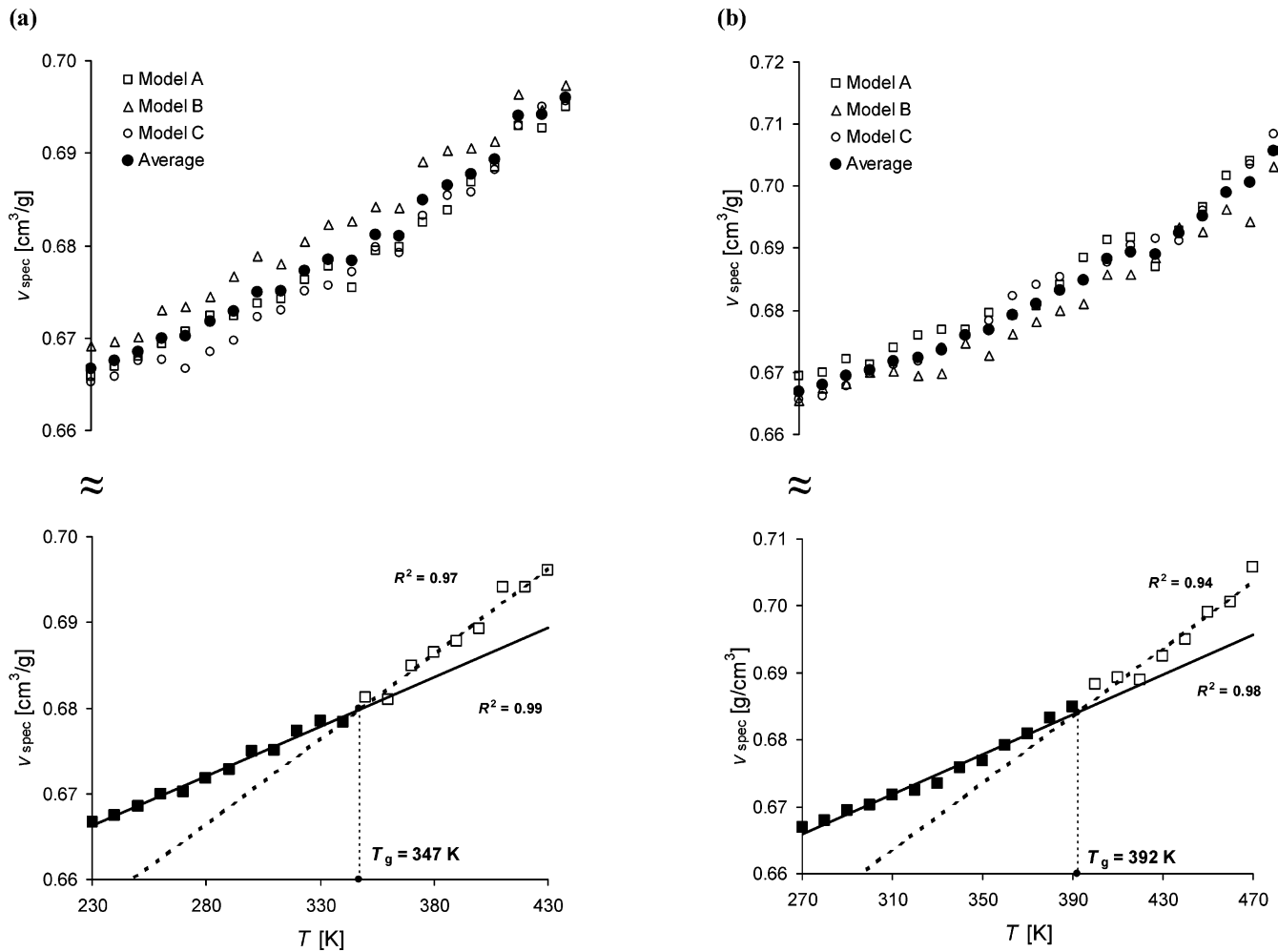


Figure 4. Calculated ν_{spec} vs T plots of (a) sucrose and (b) trehalose. Symbols are as in Figure 3.

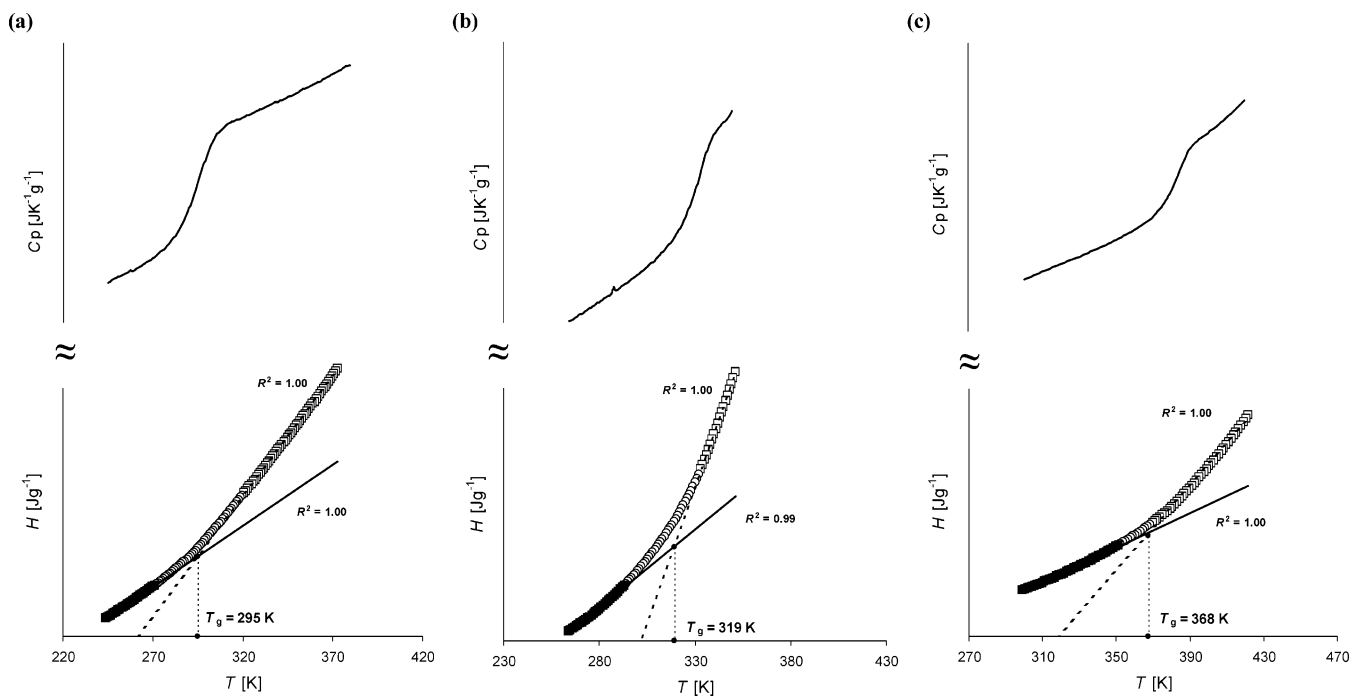


Figure 5. Experimental DSC traces of (a) glucose, (b) sucrose, and (c) trehalose. Upper plot: DSC cooling trace, C_p vs T . Lower plot: Integral of the DSC trace, H vs T (both ordinates in arbitrary units). Fit of two linear regression lines through the data points of the glass branch (■) and the data points of the rubber branch (□). T_g values are indicated at their intersection. All data points which were not used for fitting the regression lines are indicated with ○.

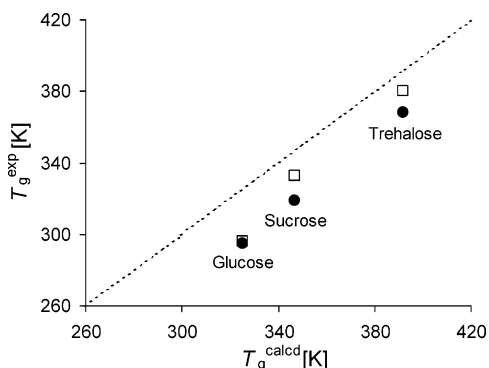


Figure 6. Both experimental T_g values plotted vs calculated T_g^{calcd} values: $T_g^{\text{mid}}/T_g^{\text{calcd}}$ (open symbols) and $T_g^{\text{cool}}/T_g^{\text{calcd}}$ (closed symbols).

overshoot in the glass transition region. Regardless of shape, both types of curves yield the same T_g .

For each of the three sugars, the experimental DSC cooling traces and the corresponding integrals (Figure 5, upper and lower plots) are shown. The regression lines employed to determine the glass transition temperature are shown in the H vs temperature plots, and the T_g values are indicated: 295, 319, and 368 K for glucose, sucrose, and trehalose, respectively.

Table 1 compares the experimental T_g^{mid} and T_g^{cool} as well as the calculated T_g^{calcd} values, and additionally, both the experimental values are plotted against the calculated ones (Figure 6). The experimental sequence of the T_g values has been

TABLE 1: Measured and Calculated Glass Transition Temperatures (K)

	glucose	sucrose	trehalose
T_g^{mid}	296	333	380
T_g^{cool}	295	319	368
T_g^{calcd}	325	347	392

correctly modeled: $T_g^{\text{glucose}} < T_g^{\text{sucrose}} < T_g^{\text{trehalose}}$. The T_g^{mid} of glucose is 1 K above its T_g^{cool} , whereas the T_g^{mid} values of sucrose and trehalose are 12 and 14 K above their T_g^{cool} values, respectively. The calculated T_g values of glucose, sucrose, and trehalose are 29, 14, and 12 K above their corresponding T_g^{mid} values and 30, 28, and 24 K above their corresponding T_g^{cool} values. As expected, MD simulations always overestimate the calculated T_g values with respect to both the experimental T_g^{mid} and T_g^{cool} values due to the extremely fast cooling rates. Nevertheless, the results of the MD calculations are satisfying due to the correct prediction of the sequence of T_g values and incremental changes between the individual T_g values.

3.3. Cooling vs Heating in Simulating Glass Transition Temperatures of Glucose. In principle, it should not matter if the v_{spec} vs T plot is obtained from a modeled heating or cooling run. Generally, as glass transition phenomena are often studied in connection with polymer systems comprising large molecules, cooling runs are preferred to heating runs as relaxation phenomena are faster at higher temperature. Therefore, it is preferable to start with a high temperature to give the long polymer chains sufficient time to relax.⁷ For small molecules such as glucose and both the disaccharides sucrose and trehalose,

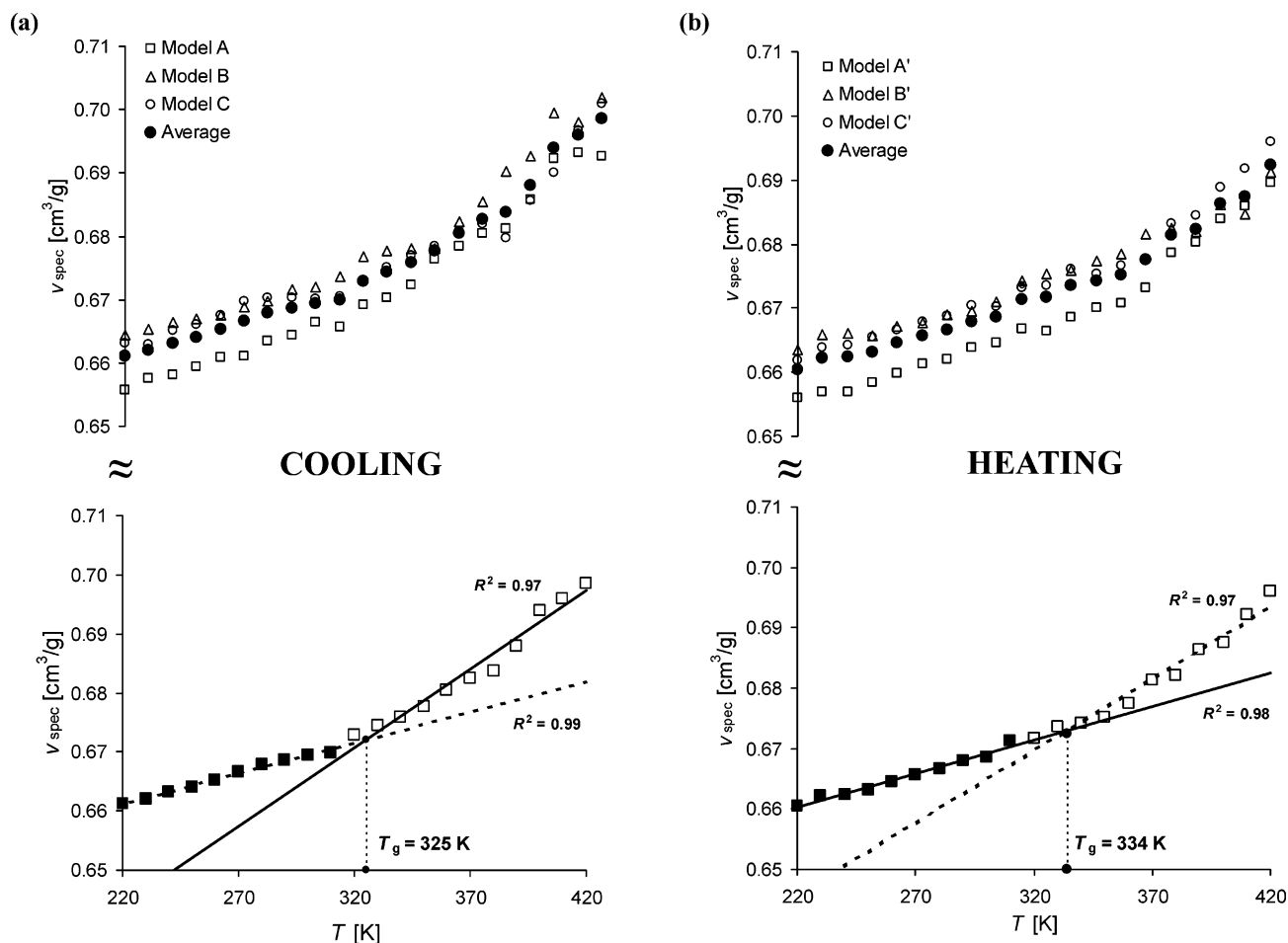


Figure 7. Calculated v_{spec} vs T plots of glucose from a modeled cooling (a) and from a modeled heating (b) cycle. Upper plots: v_{spec} data of three independent models of amorphous glucose (open symbols) along with average v_{spec} data (closed symbols). Lower plots: fit of two linear regression lines through the v_{spec} data points of the glass branch (■) and the data points of the rubber branch (□). T_g values are indicated at their intersection.

however, the relaxation process may well be sufficiently fast at lower temperatures.

To check this, in the case of glucose, a cooling cycle and a heating cycle have been performed, and both the T_g values have been determined following the procedure described in section 3.1. The specific volumes of three independent models obtained from the cooling and heating runs are plotted against temperature in the upper plots of Figure 7 (open symbols) along with the corresponding average specific volumes (closed symbols). The average v_{spec} data vs temperature plots look fairly similar for both cooling and heating data. The cooling cycle resulted in a T_g of 325 K and the heating cycle a T_g of 334 K, which are only 9 K apart. Therefore, for amorphous compounds consisting of small molecules such as glucose, the calculated T_g values can be modeled both from a cooling and a heating cycle, although a cooling cycle seems to be preferable (slightly smaller overestimation of T_g). Furthermore, it is sensible to opt for the same method used in experiment when a comparison between experimental and calculated T_g values is an issue.

4. Conclusions

Molecular dynamics software proves to be a successful tool in predicting glass transition temperatures of carbohydrates. Specific volumes of amorphous models (NPT ensembles) were successfully calculated, and their dependency on temperature was monitored in so-called cooling cycles. The scattering of calculated v_{spec} data especially in the higher temperature range (i.e., the rubbery state) makes it necessary to use at least three independent models to estimate one set of average v_{spec} data to obtain a T_g . The region where the glass transition happens is ambiguous, and data cannot be easily allocated to either the glassy or the rubbery states of the amorphous system. Two regression lines were gradually fitted starting with data from the low- and high-temperature ranges, respectively, until all data could be allocated to either the glassy or rubbery state. The calculated glass transition temperatures (T_g^{calcd}) could then be identified by the intersections of these regression lines.

Plots of the integrals of experimental DSC cooling traces vs temperature result in curves with a change in slope in the glass transition region. Similarly to the calculated v_{spec} vs temperature plots, the experimental glass transition temperatures T_g^{cool} can be obtained by simply fitting linear regression lines through the low- and high-temperature ends of these integral vs temperature curves. Furthermore, the resemblance of “calculated” and “experimental” plots allows an immediate graphical comparison between *real* and modeled T_g . Experimental T_g^{mid} values as obtained from DSC heating traces proved to be less reliable for comparison to the calculated glass transition temperatures.

An additional study on glucose regarding the difference or similarity between the modeling of a cooling or heating run of an amorphous model to obtain a T_g resulted in both methods showing comparable results. However, it is preferable to model cooling under isobaric–isothermal conditions as the experimental values also stem from DSC cooling traces.

The trend of the experimental T_g values was calculated correctly (i.e., $T_g^{\text{glucose}} < T_g^{\text{sucrose}} < T_g^{\text{trehalose}}$) with the modeled values above the experimental T_g values due to much faster cooling rates in the MD simulations. Further, the incremental changes between the experimental T_g values were satisfyingly

calculated, which raises expectations that also changes in T_g of carbohydrate excipient blends can be calculated with respect to their mixing ratio. Thus, modeling could be effectively used to tailor an optimal excipient for pharmaceutical purposes.

Acknowledgment. We thank Pfizer Inc. for financial support and Dr. G. Day (Department of Chemistry, University of Cambridge, U.K.) and Prof. A. Windle (Department of Materials and Metallurgy, University of Cambridge, U.K.) for helpful discussions.

References and Notes

- (1) Li, Y. *Adv. Drug Delivery Rev.* **2001**, *48*, 27.
- (2) Craig, D. Q. M.; Royall, P. G.; Kett, V. L.; Hopton, M. L. *Int. J. Pharm.* **1999**, *179*, 179.
- (3) Hancock, B. C.; Zografi, G. *J. Pharm. Sci.* **1997**, *86*, 1.
- (4) Hatley, R. H. M.; Blair, J. A. *J. Mol. Catal. B: Enzym.* **1999**, *7*, 11.
- (5) Crowe, J. H.; Carpenter, J. F.; Crowe, L. M. *Annu. Rev. Physiol.* **1998**, *60*, 73.
- (6) Surana, R.; Pyne, A.; Suryanarayanan, R. *Pharm. Res.* **2004**, *21*, 867.
- (7) Wagner, K. G.; Maus, M.; Kornherr, A.; Zifferer, G. *Chem. Phys. Lett.* **2005**, *406*, 90.
- (8) Yu, K.-Q.; Li, Z.-S.; Sun, J. *Macromol. Theory Simul.* **2001**, *10*, 624.
- (9) Yang, L.; Srolovitz, D. J.; Yee, A. F. *J. Chem. Phys.* **1999**, *110*, 7085.
- (10) Fried, J. R.; Ren, P. *Comput. Theor. Polym. Sci.* **1999**, *9*, 111.
- (11) Han, J.; Gee, R. H.; Boyd, R. H. *Macromolecules* **1994**, *27*, 7781.
- (12) Watt, S. W.; Chisholm, J. A.; Jones, W.; Motherwell, S. *J. Chem. Phys.* **2004**, *121*, 9565.
- (13) Chen, W.; Lickfield, G. C.; Yang, C. Q. *Polymer* **2004**, *45*, 1063.
- (14) Yoshioka, S.; Aso, Y.; Kojima, S. *Pharm. Res.* **2003**, *20*, 873.
- (15) Mazeau, K.; Heux, L. *J. Phys. Chem.* **2003**, *107B*, 2394.
- (16) Momany, F. A.; Willet, J. L. *Biopolymers* **2002**, *63*, 99.
- (17) Ekdawi-Sever, N. C.; Conrad, P. B.; de Pablo, J. J. *J. Phys. Chem.* **2001**, *105A*, 734.
- (18) Conrad, P. B.; de Pablo, J. J. *J. Phys. Chem.* **1999**, *103A*, 4049.
- (19) Caffarena, E. R.; Grigera, J. R. *Carbohydr. Res.* **1997**, *300*, 51.
- (20) Caffarena, E.; Grigera, J. R. *J. Chem. Soc., Faraday Trans.* **1996**, *92*, 2285.
- (21) Kilburn, D.; Claude, J.; Schweizer, T.; Alam, A.; Ubbink, J. *Biomacromolecules* **2005**, *6*, 864.
- (22) Wang, H.; Ansems, P.; Chum, S. P.; Hiltner, A.; Baer, E. *Polym. Mater. Sci. Eng.* **2004**, *91*, 457.
- (23) Cohen, M. H.; Grest, G. S. *Phys. Rev. B* **1979**, *20*, 1077.
- (24) Williams, M. L.; Landel, R. F.; Ferry, J. D. *J. Am. Chem. Soc.* **1955**, *77*, 3701.
- (25) Paluch, M.; Casalini, R.; Roland, C. M. *Phys. Rev. B* **2002**, *66*, 092202.
- (26) Ferrer, M. L.; Lawrence, C.; Demirjian, B. G.; Kivelson, D.; Alba-Simionesco, C.; Tarjus, G. *J. Chem. Phys.* **1998**, *109*, 8010.
- (27) Floudas, G.; Mpoukouvalas, K.; Papadopoulos, P. *J. Chem. Phys.* **2006**, *124*, 074905.
- (28) Buchholz, J.; Paul, W.; Varnik, F.; Binder, K. *J. Chem. Phys.* **2002**, *117*, 7364.
- (29) Cernošek, Z.; Holubová, J.; Cernošková, E. *Solid State Sci.* **2003**, *5*, 1087.
- (30) Allen, F. H. *Acta Crystallogr.* **2002**, *B58*, 389.
- (31) Bruno, I. J.; Cole, J. C.; Edgington, P. R.; Kessler, M.; Macrae, C. F.; McCabe, P.; Pearson, J.; Taylor, R. *Acta Crystallogr.* **2002**, *58B*, 389.
- (32) *Materials Studio 2.2*; Accelrys Inc.: San Diego, 2002.
- (33) Bunte, S. W.; Sun, H. *J. Phys. Chem.* **2000**, *104B*, 2477.
- (34) Sun, H. *J. Phys. Chem.* **1998**, *102B*, 7338.
- (35) Sun, H. *Macromolecules* **1995**, *28*, 701.
- (36) Hwang, M. J.; Stockfisch, T. P.; Hagler, A. T. *J. Am. Chem. Soc.* **1994**, *116*, 2515.
- (37) Andersen, H. C. *J. Chem. Phys.* **1980**, *72*, 2384.
- (38) Moynihan, C. T. *Rev. Mineral.* **1995**, *32*, 1.
- (39) Surana, R.; Pyne, A.; Rani, M.; Suryanarayanan, R. *Thermochim. Acta* **2005**, *433*, 173.
- (40) Ediger, M. D. *J. Phys. Chem.* **1996**, *100*, 13200.
- (41) Hay, J. M. *Pure Appl. Chem.* **1995**, *67*, 1855.